Shiraz University

Iran Agricultural Research

Journal homepage: https://iar.shirazu.ac.ir/?lang=en

Research Article

Micromorphological studies of long-term paddy rice cultivation: Emphasis on Fe-Mn sesquioxide pedofeatures

Soheila Sadat Hashemi[a*], Zahra Pourakbari[a], Saeid Hojati[b]

[a] Department of Soil Science, Faculty of Agriculture, Malayer University, Malayer, I. R. Iran
[b] Department of Soil Science, Faculty of Agriculture, Shahid Chamran University of Ahvaz, Ahvaz, I. R. Iran

ARTICLE INFO

Keywords:
B-Fabric microstructure
Rice
Voids

Received: 17 September 2025
Revised: 18 December 2025
Accepted: 21 December 2025

ABSTRACT- Rice is a major agricultural crop cultivated under conditions of prolonged flooding and water saturation. This study aims to investigate the morphology and micromorphology of paddy field soils and to examine the effects of waterlogging on soil characteristics, with particular emphasis on Fe–Mn sesquioxide features. The study area, covering approximately 75,000 hectares, is the Silakhor Plain located in the northeastern part of Lorestan Province, Iran. Landforms in the region include hills, piedmont plains, fans, floodplains, alluvial plains, and lowlands. The primary land uses are pasture and agriculture. Rice is the dominant crop, followed by alfalfa as the second most prevalent crop. Morphological, physicochemical, and micromorphological properties were investigated in seven representative pedons cultivated with rice and located in the floodplain and alluvial plain. After description and sampling, the soils were classified as Inceptisols according to Soil Taxonomy. Physical and chemical analyses showed that long-term rice cultivation increased the clay content of the surface horizons in all soil pedons and reduced soil cation exchange capacity (CEC). The dominant pedofeatures consisted of Fe–Mn sesquioxide coatings and hypocoatings, which increased in abundance with depth and covered much of the soil matrix. Other sesquioxide pedofeatures included loose discontinuous, dense complete, and dense incomplete infillings within voids and along channel walls. Redox pedofeatures were identified where oxidized Fe and/or Mn accumulated in the matrix as nodules or as Fe/Mn oxide hypocoatings or coatings along voids or coarse mineral grains, resulting from changes in the oxidation state of these elements. Calcite nodules of micrite size (< 5 μm), exhibiting typical and geodic fabrics, were also observed and were predominantly impregnated with Fe oxides. The results showed that most voids were planar, followed by channel and chamber voids, respectively, and that the quantity of voids decreased with increasing depth. Continuous rice cultivation was found to negatively affect soil structure and reduce porosity. Therefore, an alternating cultivation system is recommended to improve soil quality and maintain sustainable productivity.

INTRODUCTION

Micromorphology in soil science refers to the study of soils and related materials in their undisturbed state at the microscopic level. Its aim is to identify the processes responsible for the formation and evolution of soils in general, or of specific features, whether natural (e.g., clay skins and nodules) or artificial (e.g., irrigation crusts and plow pans) (Stoops, 2003). Paddy soils are primarily found on alluvial lands such as deltas, floodplains of large rivers, coastal plains, alluvial fans, and lower terraces. Approximately 82 million hectares of paddy land are cultivated for rice annually in these regions worldwide (Kawaguchi and Kyuma, 1974). Although some areas under rice cultivation are planted twice per year, such cases represent only a small proportion (Kawaguchi and Kyuma, 1974; Nakao et al., 2015; Afzaal et al., 2018). A characteristic feature of wetland rice cultivation is the presence of a layer of standing water in the field. The term refers to a specific soil condition describing land used for rice cultivation that remains submerged under waterlogged conditions for extended periods (Witt and Haefele, 2005). For rice cultivation, soils are kept submerged for part of the year; consequently, the micromorphological characteristics of paddy soils reflect changes induced by alternating submergence and drainage (Lee et al., 2014; Raheb and Heidari, 2023). Kawaguchi and Kyuma (1974) concluded that the process of gleying does not transform the microfabric but instead results in plasma washing and grey coloration, corresponding to the removal of iron oxides. Changes in cultivated land, crop type, and agricultural practices can alter the size, shape, and connectivity of soil pores, thereby affecting soil microstructure (Kilfeather and Vandermeer, 2008). Numerous studies have examined iron

*Corresponding Author: Assistant Professor, Department of Soil Science, Faculty of Agriculture, Malayer University, Malayer, I. R. Iran
E-mail address: s.hashemi@malayeru.ac.ir
DOI:10.22099/iar.2026.54297.1711

and manganese pedofeatures in soils, which are influenced by various environmental factors and also affect the availability of certain nutrients (Gasparatos et al., 2019; Huang et al., 2023; Raheb and Heidari, 2023).

Regarding the formation and behavior of Fe–Mn oxide coatings, studies have shown that these pedofeatures are influenced by several environmental factors, including climate (Khokhlova et al., 2021), landform (Huang et al., 2018), land use type (Raheb and Heidari, 2023), and the occurrence of Fe and Mn oxides within soil voids (Huang and Wang, 2023). Variations in these features are mainly attributed to the differences in soil redox conditions and drainage status. Wu et al. (2024) demonstrated that long-term rice cultivation over more than 2,000 years significantly affects both the biological and abiotic components of the soil iron cycle. Iron–manganese nodules are characteristic features of waterlogged soils and often display an inverse elemental distribution within the concretion ring. Manganese tends to concentrate in the inner part of the nodule, whereas iron accumulates along the outer edges. This pattern reflects alternating wet and dry periods and fluctuations in oxidation–reduction conditions during the formation of Fe–Mn nodules (Huang et al., 2023). In rice field soils, Zhuang et al. (2025) identified iron and clay coatings with a cementation structure, referred to as depleted clay coatings. These pedofeatures are commonly associated with high groundwater tables and prolonged waterlogging. Their observations also showed that iron nodules frequently occur along plant roots in thin sections, whereas manganese nodules are generally less abundant. Land-use change has also been shown to influence soil micromorphological features. Khokhlova et al. (2021) reported that the conversion of forest land to arable land resulted in the formation of two types of hard carbonate nodules. In soils under corn cultivation and bare fallow within the Bck horizon, the micromass consisted of iron–clay material slightly impregnated with fine carbonates, producing a crystallitic b-fabric. Similarly, Raheb and Heidari (2023) compared paddy and non-paddy soils and found that soils under kiwi cultivation had greater pore volume than paddy soils due to the unsaturated conditions and higher biological activity in the upper horizons. Their results also indicated that converting paddy fields to kiwi orchards increased soil porosity and promoted the formation of more crystallized iron forms, which can be attributed to the enhanced microbial activity under non-saturated conditions. In addition, they reported higher concentrations of DTPA-extractable iron and manganese in rice fields, whereas phosphorus and potassium levels were lower compared with soils cultivated with kiwi and citrus. Iron and manganese sesquioxides in the soil matrix can influence the availability and uptake of nutrients, particularly phosphorus. Therefore, understanding their abundance and spatial distribution across different landforms, land uses, and cropping systems is important for effective soil and farm management. Over long cultivation periods, these soil-forming processes become increasingly pronounced under the influence of various environmental and management factors. The present study focuses on soils in an area that has been cultivated with rice for approximately 50 years. Continuous rice cultivation under flooded conditions may have altered the micromorphological pedofeatures of the soil, particularly Fe–Mn sesquioxides. Accordingly, the objective of this study is to explore the changes in soil micromorphological characteristics resulting from long-term rice cultivation and to evaluate the associated impacts on soil properties.

MATERIALS AND METHODS

Field sampling

The study area covered approximately 75,000 hectares in the Silakhor Plain, located in the northeastern part of Lorestan Province in western Iran (Fig. 1). The mean annual rainfall and temperature were 679 mm and 16.1 °C, respectively. According to Banaei (1998), the soil moisture and temperature regimes were classified as xeric and thermic, respectively. Based on the geomorphological map (Fig. 2), the area consisted of several landforms: hills covering 23% (27,900 ha), floodplains 5.3% (6,500 ha), piedmont plains 34.2% (41,600 ha), lowlands with gentle slopes 8% (9,800 ha), alluvial fans 6% (7,200 ha), and alluvial plains 23.3% (28,400 ha). In terms of geology and parent materials, the Silakhor Plain was mainly composed of Quaternary deposits, including conglomerates and young alluvium in the central areas. The surrounding highlands consisted of folded and, in some places, fractured sedimentary masses of limestone belonging to the Surmeh Formation. In addition, gray-colored Jurassic and Cretaceous limestones occurred in the higher elevations. For this study, land use and vegetation maps were first examined, after which seven representative soil pedons were excavated and described. Most of the pedons were located in floodplains and alluvial plains where rice was cultivated. Soil samples from different horizons were collected for macromorphological and micromorphological analyses (Fig. 2). Rice has been the dominant crop in the region for more than 50 years, while alfalfa is the second most common crop. Photographs of several representative pedons are presented in Fig. 3.

Physical and chemical properties

Soil samples were collected from both surface and subsurface horizons. Particle-size distribution was determined using the method of Gee and Bauder (1986). Organic carbon content was measured following Nelson and Sommers (1996), while calcium carbonate equivalent (CCE) and gypsum contents were determined according to Allison and Moodie (1965) and Loppert and Suarez (1996), respectively. Soil pH was measured in a saturated paste using a glass electrode (Thomas, 1996), and electrical conductivity (EC) was determined following the procedure of Rhoades (1996). Cation exchange capacity (CEC) was measured using sodium acetate at pH 8.2 (Chapman, 1965). Soil organic matter content was calculated by multiplying the organic carbon content by a factor of 1.724. Soil pedons were described and classified according to the Soil Survey Manual (2017) and the Keys to Soil Taxonomy (Soil Survey Staff, 2022).

Micromorphology study

For micromorphological analysis, 18 thin sections were prepared from undisturbed clods collected from eleven different soil horizons. The thin sections, approximately 70

cm² in area and 30 µm thickness, were prepared from air-dried, undisturbed, and oriented clods using standard procedures described by Murphy (1986). The prepared thin sections were examined using polarizing microscopes (Hund Wetzlar, Nikon DS-FI, and Leitz Ortholux II POL BK) under plane-polarized light (PPL) and crossed-polarized light (XPL). Descriptions and micromorphological feature analyses were aligned with the terminology and guidelines proposed by Stoops (2003).

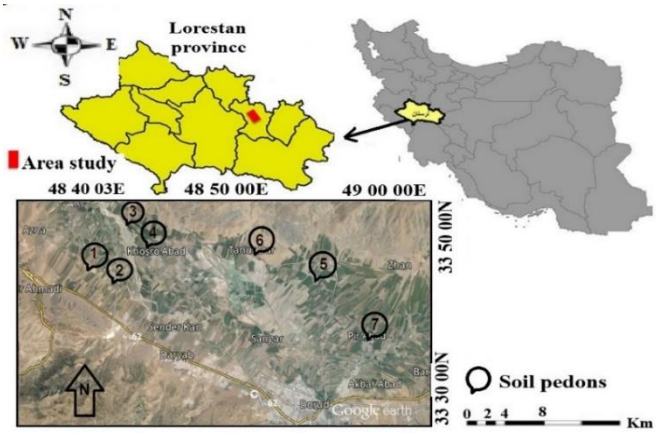

Fig. 1. Location of the study area on the map of Iran, showing soil sampling sites on Google Earth (2022).

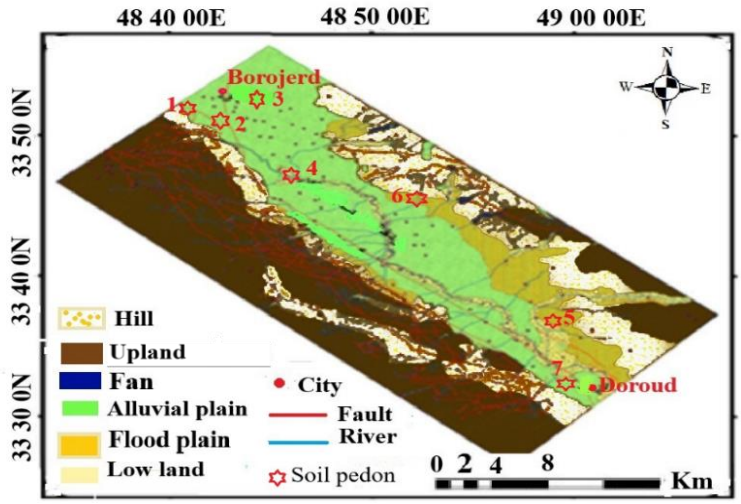

Fig. 2. Geomorphological map of the study area.

Fig. 3. Soil pedons are located in the (a) floodplain (Pedon 4), (b) alluvial plain (Pedon 7), and (c) alluvial plain (Pedon 3) landforms.

RESULTS AND DISCUSSION

Physical and chemical properties

Some morphological properties and physicochemical characteristics of the seven pedons are presented in Table 1 and Table 2, respectively. Soil color ranged from 2.5YR to 10YR, which is typical for paddy soils. Profile observations showed that most soils exhibit brown colors in the surface horizons and gray colors in the lower horizons. Secondary carbonates were evident in most profiles and were commonly observed in the form of mycelium. The soils displayed massive, granular, angular blocky, and subangular blocky structures and were classified as Typic Epiaquepts according to Soil Taxonomy. In general, soil texture was heavy, predominantly within the clay class. Continuous waterlogging conditions may therefore contribute to the development of heavier soil textures. The increase in clay content with depth suggests clay translocation, whereby clay particles are leached from upper horizons and accumulate in lower layers. Some studies attribute the heavy texture of paddy soils to the factors such as the presence of fine particles in irrigation water and increased soil degradation caused by decomposition processes and puddling operations (Cheng et al., 2009; Lee et al., 2013). Soil pH ranged from 6.8 to 7.9. In some pedons, pH decreased with increasing soil depth. Waterlogging generally increases the pH of acidic soils while decreasing pH in alkaline soils (Ponnamperuma, 1978). CEC ranged from 10.2 to 29.8 cmolc kg^{-1}. Both the level of organic matter and the type of clay mineralogy influence CEC (Hashemi and Asadi, 2018). Results reported by Hashemi and Asadi (2018) for the same region indicated that the dominant clay minerals are smectite and vermiculite, both of which contribute to the higher CEC values. Organic matter was mainly concentrated in the surface horizons and decreased markedly with increasing soil depth in all pedons.

The development of waterlogged conditions, together with the accumulation of rice residues, are the main factors contributing to the high organic matter content in the surface horizons (Fig. 4) (Hashemi and Asadi, 2018). Rice cultivation under anaerobic conditions created by prolonged flooding promotes the accumulation of organic matter, particularly in the upper soil layers. Consequently, paddy soils act as important reservoirs of soil organic carbon within terrestrial ecosystems (Xia et al., 2017; Chen et al., 2021). Nakatsuka and Tamura (2016), in a study of paddy rice fields without manure application, reported a strong correlation between CEC and organic carbon. Similarly, Linh et al. (2015), in their investigation of upland crops within rice rotation systems, demonstrated improvements in soil chemical quality under cropping systems that included rotations of rice with mung bean or maize grown on temporary beds. These systems resulted in increased soil organic carbon and a presumed hydrolysable labile carbon fraction compared with continuous rice monoculture. Only minor changes in soil salinity were observed in the study area. Due to the relatively high annual rainfall and the artificial flooding associated with rice cultivation, gypsum content was negligible. However, the calcareous nature of the parent materials resulted in a relatively high CCE content (up to 24.8%), which was considerably higher than the gypsum content. In most soil profiles, CCE content increased with depth. The high groundwater level and periodic flooding of the topsoil have created specific environmental conditions that strongly influence soil formation in the region. Since climatic conditions are relatively uniform across the study area, little variation was observed in soil classification and development. Color analysis of the soil pedons showed that most profiles have brown surface horizons and gray subsurface horizons. The gray coloration indicates reducing conditions typical of paddy soils (Gasparatos et al., 2019). Based on the results of physical and chemical analyses, together with the regional moisture and temperature regimes and field observations of the excavated pedons, the soils of the study area were classified as Inceptisols according to Soil Taxonomy (Soil Survey Staff, 2022).

Micromorphological study

Micromorphological analysis included a general micropedological description of soils cultivated under rice monoculture and rice–alfalfa rotation systems. The results of the thin-section descriptions are presented in Table 3. In all Ap horizons, the ped type is predominantly massive to granular and generally partially accommodated (Fig. 5e). Most of the voids in the Ap horizons consist of compound packing voids and planar voids, while vughs were occasionally observed. Accordingly, the microstructure of the Ap horizons can be described as massive with a complex void system. The amount of decomposing root material at this depth was relatively low, approximately 2–3%. One of the most prominent matrix pedofeatures observed in the pedons was depletion, which indicates the presence of surface waterlogging conditions (Zhuang et al., 2025) (Fig. 5a and Fig. 5b). These pedofeatures develop under reducing chemical conditions within the soil matrix compared with the surrounding S-matrix.

The distribution pattern in the surface (Ap) horizons is predominantly double-spaced porphyric and, less commonly, porphyric (Fig. 5c), indicating a dominance of fine material surrounding coarser grains. Similar distribution patterns have been reported by Vera et al. (2007) and Zhuang et al. (2025). Hypocoatings and quasicoatings of Fe oxides are additional pedofeatures identified in the Ap horizons. These features commonly occur along channel walls and around voids (Fig. 4d), reflecting localized redox processes associated with periodic saturation and aeration. Birefringence in the Ap horizons is crystalline, attributable to the presence of fine mineral particles such as quartz, feldspar, and calcite (Fig. 5). The clay-to-fine particle (c/f) ratios in all Ap horizons are typically around 2:8, indicating the predominance of fine particles within the groundmass (Fig. 5). In the Bkg horizons of pedons 1 and 2, both massive and subangular blocky peds were observed. The dominant void types in this horizon include planar and chamber voids, with occasional vughs (Fig. 6a, Fig. 6b, and Fig. 6c). With increasing depth and prolonged waterlogged conditions, the number of channels decreased, likely due to the shallow rooting depth and reduced biological activity (Kemp et al., 2004; Raheb and Hydari, 2023). Pedofeatures in the Bkg horizon include

iron coatings around channels and quasicoatings along root traces (Fig. 6a). Iron coatings were also observed surrounding carbonate nodules (Fig. 6c), most of which appear to have formed *in situ*. Kowalska et al. (2020), in their study of calcium carbonate-rich sediments, similarly reported diffusely bordered Fe–Mn nodules in thin sections. These nodules were predominantly formed *in situ* rather than being transported, indicating specific precipitation dynamics and hydrological conditions in such environments.

Table 1. Morphological properties of the pedons

Pedon No. (Landforms)	Horizon	Depth (cm)	Soil color (moist)	Structure	Boundary	Identifiable characteristics
1 (Flood Plain) (Typic Epiaquepts)	Apg	0-20	10YR5/2	Massive	Regular	Root residual of crops
	Bkg	20-50	7.5YR4/2	Angular Blocky	Diffuse	Secondary carbonate (mycelium form > 5%)
	Bk1	50-78	7.5YR4/3	Subangular Blocky	Diffuse	Secondary carbonate (mycelium > 5%), > 15% fine gravel
	Bk2	78-118	7.5YR4/3	Subangular Blocky	-	Secondary carbonate (> 5%), > 15% coarse gravel
2 (Alluvial Plain) (Typic Epiaquepts)	Apg	0-12	5YR5/1	Subangular	Diffuse	Gley
	Bkg1	12-57	5YR5/2	Angular Blocky	Regular	Secondary carbonate (powder form > 5%), Redoximorphic features
	Bkg2	57-110	5YR4/2	Angular Blocky	Diffuse	Secondary carbonate (powder form > 5%), Redox condition
3 (Alluvial Plain) (Typic Epiaquepts)	Apg	0-21	10YR5/1	Massive	Diffuse	Fine gravel > 10%
	Bk1	21-57	2.5YR4/1	Angular Blocky	Regular	Secondary carbonate (powder form > 5%), > 15% gravel
	Bk2	57-96	2.5YR3/2	Angular Blocky	Regular	Secondary carbonate (powder form > 5%), 20-30% of gravel
	Bk3	96-130	2.5YR3/2	Subangular Blocky	Diffuse	Secondary carbonate (powder form > 5%), > 40% gravel
4 (Flood Plain) (Typic Epiaquepts)	Apg	0-27	2.5YR5/1	Subangular	Regular	Little of root residual
	Bg1	27-57	2.5YR5/2	Subangular Blocky	Regular	Fine gravel (5-10%), mottling
	Bg2	57-82	2.5YR5/3	Subangular Blocky	Diffuse	Fine gravel (5-10%), mottling
	Bkg1	82-112	2.5YR4/4	Angular Blocky	Diffuse	Secondary carbonate (mycelium form > 5%), Coarse gravel (10%)
	Bkg2	112-142	2.5YR3/4	Angular Blocky	Diffuse	Secondary carbonate (mycelium form > 5%), Coarse gravel (10%)
5 (Flood Plain) (Typic Epiaquepts)	Ap	0-12	2.5YR5/2	Massive	Diffuse	Little of root residual, No gravel
	Bg	12-44	2.5YR4/1	Angular Blocky	Regular	Fe & Mn accumulation mottle, No gravel
	Bk1	44-72	7.5YR4/3	Angular Blocky	Diffuse	Secondary carbonate (mycelium form > 5%),
	Bk2	72-102	7.5YR4/3	Subangular Blocky	Regular	Secondary carbonate (powder form > %5), fine gravel > 5%
	Bk3	102-135	10YR4/3	Subangular Blocky	-	Secondary carbonate (powder form > %5), fine gravel > 5%
6 (Flood Plain) (Typic Epiaquepts)	Ap	0-12	2.5YR4/1	Granular	Diffuse	Root residual
	Bg1	12-55	2.5YR4/2	Subangular	Regular	Gley condition
	Bg2	55-85	5YR4/3	Subangular	Regular	Gley condition
	Bg3	85-125	5YR3/3	Subangular	Diffuse	Gley condition
7 (Alluvial Plain) (Typic Epiaquepts)	Apg	0-20	10YR5/2	Massive	Regular	Root residual, Gley condition
	Bg1	20-53	10YR4/2	Angular Blocky	Diffuse	Redoximorphic feature, Gley condition
	Bg2	53-83	10YR4/3	Subangular Blocky	Diffuse	Redoximorphic feature, Gley condition
	Bg3	83-125	10YR4/3	Subangular Blocky	Diffuse	Secondary carbonate (powder form < 5%), Gley condition

Table 2. Physical and chemical properties of the pedons

Pedon No.	Horizon	Depth (cm)	Particles size distribution (%)			CCE (%)	pH	EC (dSm^{-1})	CEC ($cmol_c\ kg^{-1}$)	OM (%)	Gypsum (%)
			Sand	Silt	Clay						
1	Apg	0-20	32.5	26	41.5	24.4	7.9	0.1	22.2	2.3	0.2
(Typic Epiaquepts)	Bkg	20-50	24.5	26	49.5	24.1	7.3	0.1	18.6	0.9	0.1
	Bk1	50-78	34.5	20	45.5	24.1	7.2	0.1	20.5	0.5	0.1
	Bk2	78-118	43	19.5	37.5	24.2	6.9	0.1	14.5	0.6	0.1
2	Apg	0-12	22.5	36	41.5	17.1	7.8	0.2	29.9	2.3	0.2
(Typic Epiaquepts)	Bkg1	12-57	20.5	34	45.5	18.5	7.6	0.2	25.6	1.1	0.1
	Bkg2	57-110	23	31.5	45.5	20.7	7.2	0.2	24.8	0.9	0.04
3	Apg	0-21	50.5	22	27.5	15.3	7.6	0.1	14.5	2	0.1
(Typic Epiaquepts)	Bk1	21-57	50.5	22	27.5	14.1	7.4	0.1	14.5	1.3	0.04
	Bk2	57-96	48.5	22	29.5	15.5	7.4	0.1	15.4	1	0.04
	Bk3	96-130	54.5	20	25.5	16.1	7.7	0.1	14.5	1.3	0.04
4	Apg	0-27	28.5	42	29.5	15.5	7.9	0.2	23	1.6	0.1
(Typic Epiaquepts)	Bg1	27-57	30.5	38	31.5	15.9	6.9	0.2	15.4	1.6	0.04
	Bg2	57-82	20.5	38	41.5	18.5	7.5	0.1	17.1	0.6	0.04
	Bkg1	82-112	22.5	30	47.5	20.1	7.5	0.1	20.5	0.7	0.04
	Bkg2	112-142	25	33.5	41.5	23.4	6.9	0.2	18.8	0.6	0.04
5	Ap	0-12	35	27.5	37.5	20.8	7.7	0.2	17.1	3	0.1
(Typic Epiaquepts)	Bg	12-44	36.5	18	45.5	20.2	7.4	0.2	19.6	2.3	0.1
	Bk1	44-72	22.5	30	47.5	22.1	7.2	0.1	16.2	1.3	0.1
	Bk2	72-102	23	31.5	45.5	23	7.2	0.1	15.4	0.6	0.1
	Bk3	102-135	18.5	30	51.5	24	7.8	0.1	15.4	0.3	0.04
6	Ap	0-12	42.5	36	21.5	23.3	7.9	0.2	18.8	2.4	0.1
(Typic Epiaquepts)	Bg1	12-55	41	33.5	25.5	22.3	7.4	0.2	18	2.3	0.1
	Bg2	55-85	39	25.5	35.5	23.4	7.3	0.2	17.1	1.3	0.04
	Bg3	85-125	26.5	24	49.5	24.4	8	0.2	13.3	1.1	0.04
7	Apg	0-20	33	25.5	41.5	16.3	7.8	0.2	11.9	2.8	0.1
(Typic Epiaquepts)	Bg1	20-53	25	27.5	47.5	24.1	7.8	0.2	11.1	1.7	0.1
	Bg2	53-83	39	25.5	35.5	24.4	7.3	0.2	12	1.3	0.2
	Bg3	83-125	27	29.5	43.5	24.8	7.3	0.2	10.2	0.5	0.2

CCE: Calcium carbonate equivalent; EC: Electrical conductivity; CEC: Cation exchange capacity; OM: Organic matter.

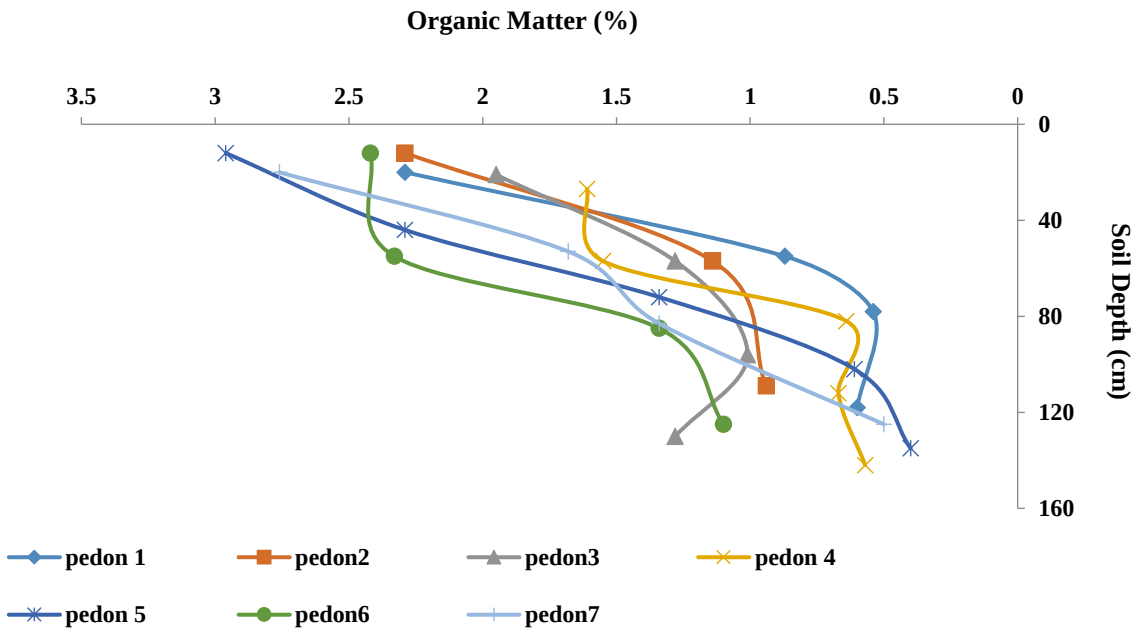

Fig. 4. Organic matter in soil pedons.

In the Apg horizon of pedon 2, fine mineral particles, such as plagioclase (Fig. 7a) and channel voids (Fig. 7b and Fig. 7c) were observed. The presence of channel voids indicates root penetration and biological activity within the soil (Kemp et al., 2004; Wu et al., 2024). As the distance from the channels increases, the oxygen concentration decreases, which reduces the rate of iron oxide precipitation. Consequently, the boundaries of the coatings become indistinct, and at greater distances the matrix appears relatively clear. This distribution pattern reflects alternating wet and dry periods and fluctuating oxidation–reduction conditions during the formation of Fe oxide coatings (Huang et al., 2023). Ayoubi et al. (2025), in a study comparing natural forest, disturbed forest, and cultivated land, demonstrated that land-use change significantly affects soil void types and microstructure. They reported that pore types such as channels and chambers, indicative of biological activity, were dominant in forest soils, whereas planar voids and vughs were more common in cultivated soils, reflecting the disruption of macro-aggregates. The yellow clay coating observed around plant roots in the thin sections represents depleted clay coatings (Fig. 7b). Considering that the study area has a xeric moisture regime, it is likely that annual rainfall promotes the leaching of clay from surface horizons and its subsequent deposition around pores in underlying layers (Zhuang et al., 2025). Clay accumulations in these sections differ from those in argillic horizons, as they are lighter in color and occur discontinuously, which is primarily attributed to alternating wet and dry conditions. Iron and manganese pedofeatures dominate most thin sections (Fig. 7c). Roquero et al. (2013), in their study of hydromorphic soils, reported that strongly iron-impregnated opaque domains may represent inherited Fe-rich nodules or clasts originally present in the parent sediments. These pedofeatures subsequently undergo iron mobilization, producing the iron depletion and accumulation domains observed at the micromorphological scale. Differential iron bleaching is not always directly associated with the fissure or pore system of the groundmass, suggesting that differential vertical fluxes of water and sediments within the soil (micro water-escape features) may enhance the formation of redoximorphic features around structural discontinuities. In the Bk1 horizon of pedon 3, the microstructure is mainly vesicular to massive. The dominant void types include vughs and vesicular voids, occupying approximately 15–20% of the matrix area (Fig. 8). The distribution pattern in this horizon is micromorphic (Fig. 8), with a c/f ratio of 1:9, indicating the dominance of fine materials in the groundmass. Approximately 15–25% of the matrix consists of mineral fragments, including quartz, plagioclase (Fig. 8a and Fig. 8b), and granite fragments (Fig. 8c). Root residues are minimal at this depth, accounting for only 1–2% of the matrix. The presence of Fe and Mn nodules with distinct boundaries, together with hypocoatings and quasi-coatings of Fe with diffuse borders, has been reported as characteristic pedofeatures of paddy soils (Yurong et al., 2008). Another notable pedofeature is the occurrence of calcite nodules impregnated with iron oxides in thin sections (Fig. 8e and Fig. 8f). Gargiulo et al. (2013), in their study on the mobilization of Fe oxides and $CaCO_3$ within soil pore systems, demonstrated that these processes can significantly modify pore size distribution. Their findings highlighted specific mechanisms of pore transformation induced by Fe and micrite pedofeatures, which form through the suspension and mobilization of Fe oxides and $CaCO_3$ within the soil matrix.

Table 3. Some micromorphological properties were studied in thin sections

Pedon. Horizon	Depth (cm)	Microstructure	Pedality	Voids	c/f related Distribution pattern	b-fabric	Organic matter type	Pedofeature
1. Apg	0-25	Granular and massive	Partially accommodation	Compound packing void	Porphyric and double porphyric, 3/7	Crystallitic	Rot root of Rice (1-2%), monomorphic	Depletion, Fe-coating around void, coating of calcite, carbonate nodule, loose infilling of Fe and carbonate
1. Bkg	25-55	Massive and sub angular blocky	Partially and moderate accommodation	Planar, chambers and vughs	Double porphyric, 2.5/7.5	Crystallitic	Rot root of Rice (1-2%), monomorphic	Fe-coating around void, coating of calcite, carbonate nodule, loose infilling of Fe and carbonate, fragment loose discontinuous infilling in voids
1. Bk1	55-118	Massive and sub angular blocky and blocky	Partially and moderate accommodation	Planar, chambers and vughs	Double porphyric, 2.5/7.5	Crystallitic	Rot root of Rice (1-2%), monomorphic	Fe-coating around void, coating of calcite, carbonate nodule, loose infilling of Fe and carbonate, fragment loose discontinuous infilling in voids
2. Apg	0-12	Massive(more), and vughs	Partially accommodation	Vughs	Double porphyric, 2/8	Crystallitic	Rot root of Rice (2-3%)	Fe coating and quasicoating around voids and roots, quasicoating of Fe around calcite nodule, coating of calcite around voids, calcite nodule, loose continuous infilling of Fe and clay in voids
2. Bkg1	57-109	Massive and some point channels	Partially accommodation	Chambers, channels and planar	Double porphyric, 2/8	Crystallitic	Rot root of Rice (2-3%)	Coating of calcite around voids, calcite nodule, Fe nodule, fragment continuous infilling
3.Bk1	21-57	Massive and vesicles	No pedality	Vugh, Compound packing voids	Fine monic, double porphyric, 1/9	Crystallitic	Rot root of Rice (1-2%), monomorphic	Fe coating and quasicoating, coating of calcite around voids, calcite nodule, loose continuous infilling of Fe and clay in voids
3.Bk2	57-96	Massive and vesicles	No pedality	Compound packing voids, vesicles	Double porphyric and porphyric, 3/7	Crystallitic	Rot root of Rice (1-2%), monomorphic	Fe coating and quasicoating around voids and roots, calcite nodule, loose continuous infilling of Fe and clay in voids
6.Bg2	55-85	Massive	Partially accommodate	Vughs and channels	Fine monic, double porphyric, 2.5/7.5	Crystallitic	Rot root of Rice (5-10%)	Clay infilling, clay impregnated of Fe, Hypo coating of sesquioxides, Fe coating, Fe nodules
6.Bg3	85-125	Massive	Partially accommodate	Planes and chambers	Fine monic, porphyric, 2.5/7.5	Crystallitic	Rot root of Rice (5-10%)	Clay infilling, clay impregnated of Fe, Hypo coating of sesquioxides, Fe coating, and quasicoating around voids, Fe nodules
7.Apg	0-20	Massive and vesicles	Moderately accommodate	Chambers and a few channels	Porphyric, 2/8	Crystallitic, stipple stickle	Rot root of Rice (2-5%)	Loose discontinuity of organic residue and Fe nodule, clay infilling, coating of calcite, calcite impregnated with Fe
7.Bg	20-83	Sub angular blocky	Moderately accommodate	Chambers and planes	Porphyric, 2/8	Crystallitic	Rot root of Rice (2-5%)	Loose discontinuity of organic residue and Fe nodule, clay infilling, coating of calcite, calcite impregnated with Fe

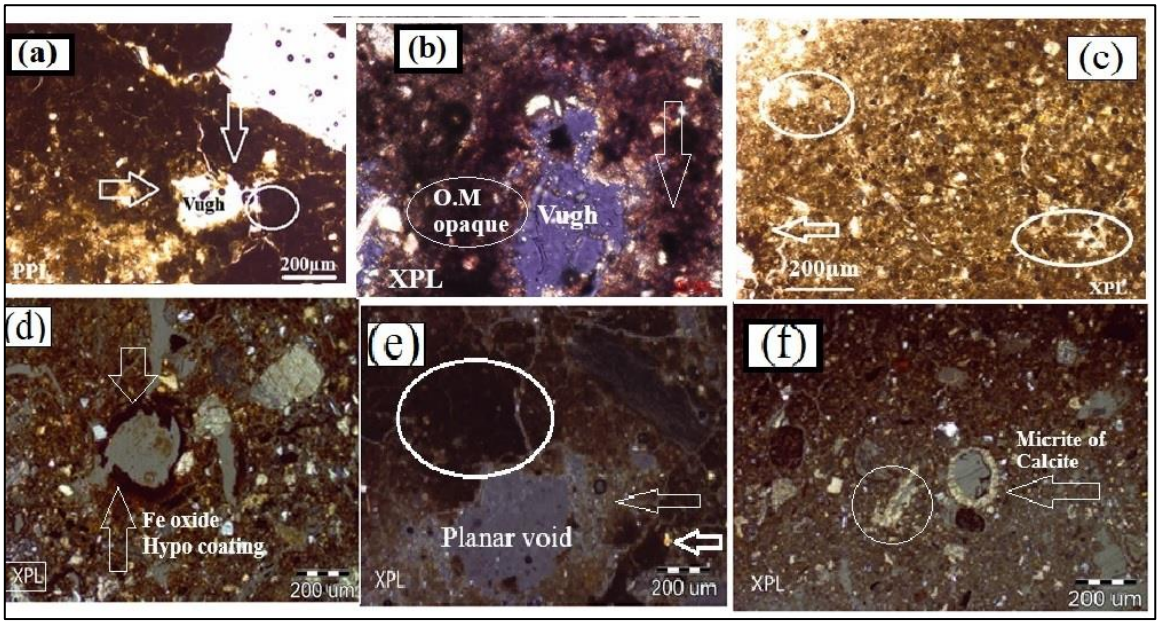

Fig. 5. (a) and (b) Depletion pedofeatures and organic material opaque accumulation in vughs voids. (c) Porphyric distribution pattern, Fe concretions and coating. (d) Hypo-coating of Fe oxide around the void. (e) Plagioclase minerals, planes voids, and subangular blocky aggregate. (f) Micrite coating of calcite around the void (Apg. Pedon 1).

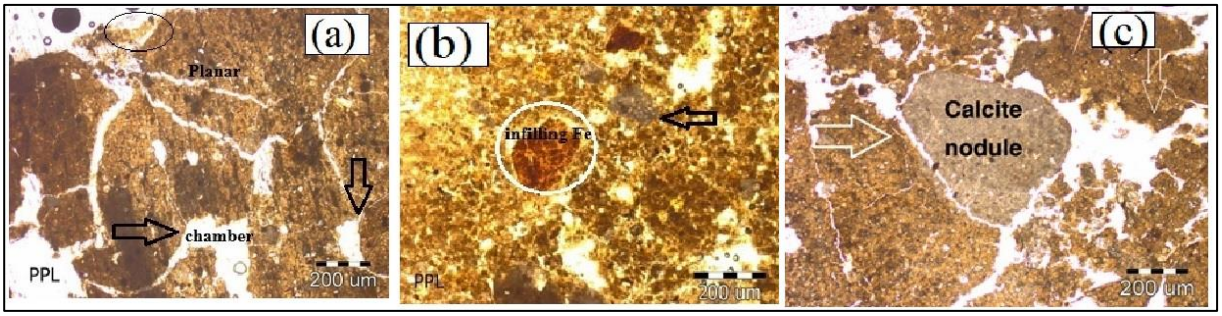

Fig. 6. (a) planar and chambers voids, residue of rotting root in void, coating of Fe oxides around voids, depletion feature. (b) Fe infilling in void, calcite nodules. (c) Calcite infilling in void, Fe concretion around voids (Bkg1. Pedon 1).

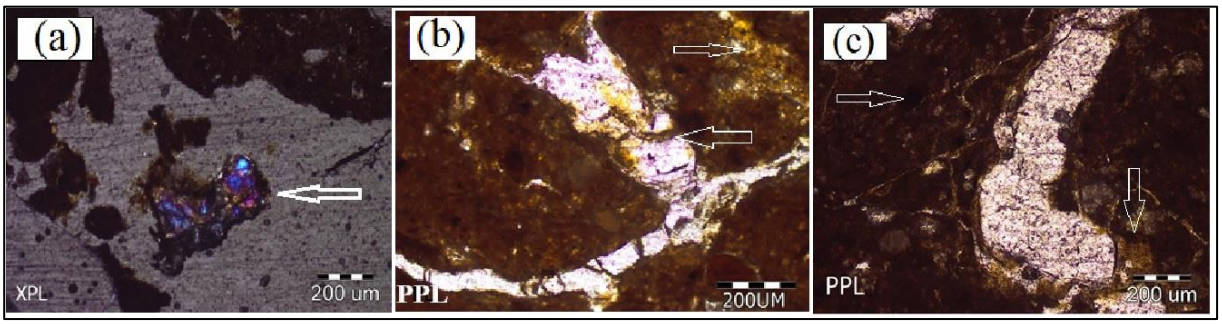

Fig. 7. (a) Plagioclase mineral. (b) Channels voids with monomorphic infilling and loose discontinuous infilling of clay and clay coating on rotting root. (c) Channels and planes void with a quasicoating of Fe-Mn oxides nodules (Apg. Pedon 2).

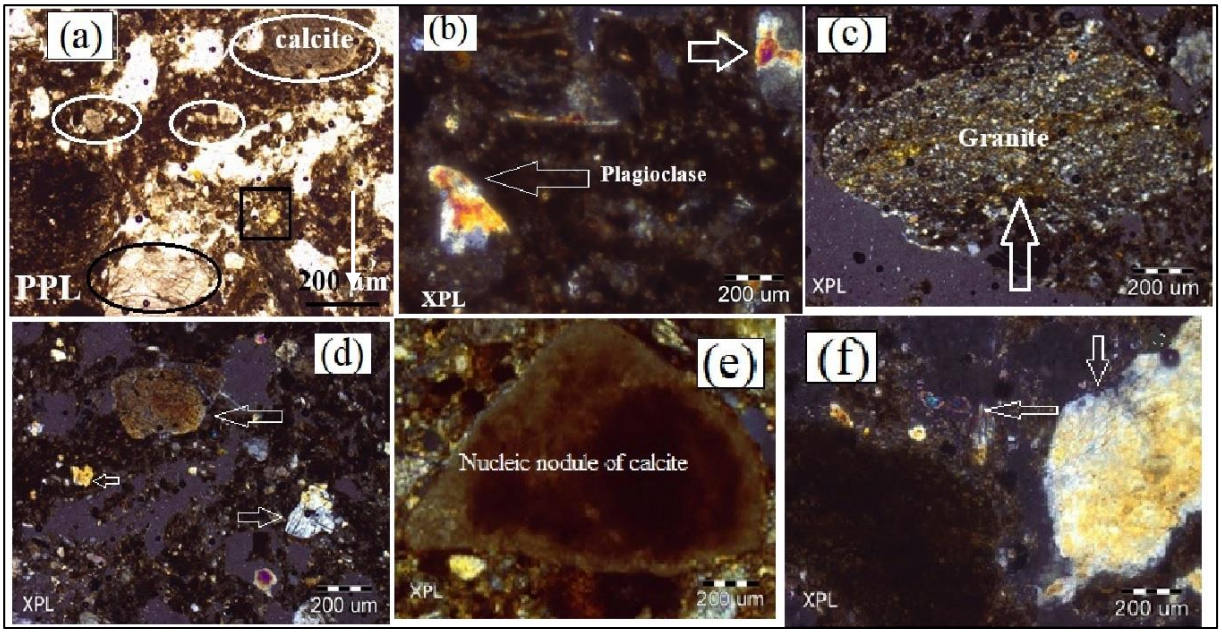

Fig. 8. (a) Calcite in a void and calcite coating on a fine particle. (b) Plagioclase minerals in voids. (c) Granite rock in S-matrix. (d) Carbonate calcium nucleic nodule, quatrz and Plagioclase minerals and vugh and vesicles voids. (e) Calcite nodule impregnated with Fe oxides. (f) Quartz, feldspar, and plagioclase minerals (Bk1. pedon 3).

In the Bg horizon of pedon 6, birefringence is crystalline and exhibits a mosaic speckled pattern (Fig. 9a and Fig. 9b). The presence of rotting roots increases at this depth, covering approximately 2–5% of the area (Fig. 9c and Fig. 9d). Iron hypocoatings mainly occur around voids and root channels (Fig. 9c). The presence of channels, with or without roots, is one of the mechanisms responsible for the formation of this type of coating. Air penetrates the channel and diffuses outward to a certain radius from the channel opening, with its concentration highest at the channel boundary. As oxygen enters the channel, divalent iron in the surrounding soil is oxidized and precipitates as iron oxides or hydroxides along the channel margins (Huang et al., 2023). Prakongkep et al. (2007), in their study of Thai paddy soils, showed that manganese oxides reflect seasonal fluctuations in the water table, which lead to alternating reducing and oxidizing conditions. In pedon 7, a granostriated b-fabric was observed. Impregnated pedofeatures consisting of Fe and Mn oxides are distinguished by their black color relative to the surrounding S-matrix (Fig. 10a–c). Other pedofeatures include Fe and calcite coatings, fine Fe nodules, and Fe infillings within voids in pedon 7 (Fig. 10a, Fig. 10b, and Fig. 10d). The results indicate that most paddy soils exhibit massive or subangular blocky microstructures. The occurrence of moderately developed structures in the surface horizons and massive structures at greater depths suggests destruction of the natural soil structure and increased compaction due to the puddling practices in paddy cultivation (Raheb and Hydari, 2023). However, with the growth and development of rice roots and the occurrence of periodic drying in the surface layer, weak structural development may gradually occur (Khokhlova et al., 2021; Ayoubi et al., 2025). Among the observed void types, planar, channel, and chamber voids were the most common, respectively, and their abundance decreased with increasing soil depth. With increasing depth and prolonged waterlogging conditions, the occurrence of channel voids declined. The presence of channel voids in soil horizons indicates root growth and penetration (Kemp et al., 2004), vertical water movement, capillary flow, and biological activity of soil organisms (Wu et al., 2024). Planar voids commonly form due to the shrinkage in clay-rich soils when field moisture decreases after extended wet periods in paddy fields. Paddy soils generally lack well-developed ped structures, and subangular blocky peds are commonly observed. Khedri et al. (2018) compared the micropedology of soils under long-term canola and sugar beet cultivation and found that the microstructure in surface horizons was mainly massive and plate-like, whereas subsurface horizons exhibited subangular or angular blocky, and sometimes spongy, structures. Their results also showed that soil microstructure was better developed under canola than under sugar beet cultivation.

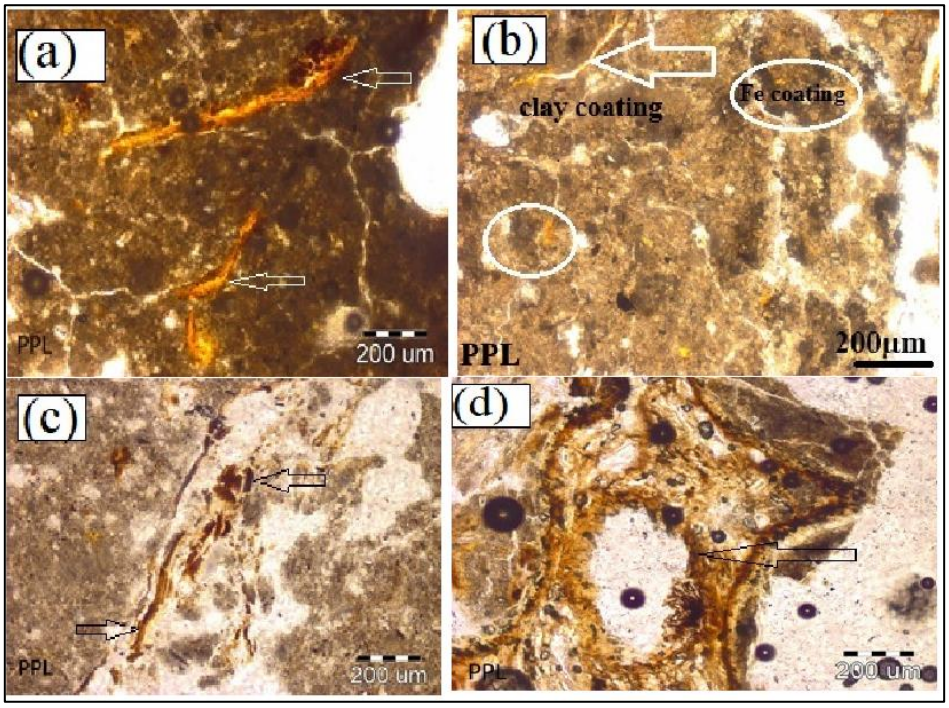

Fig. 9. (a, b) Planar voids with clay infilling and clay coating and Fe coating. (c) Root is rotting and Fe coating around it and Fe coating on the void. (d) Rotting root and Fe coating around it (Bg3. Pedon 6).

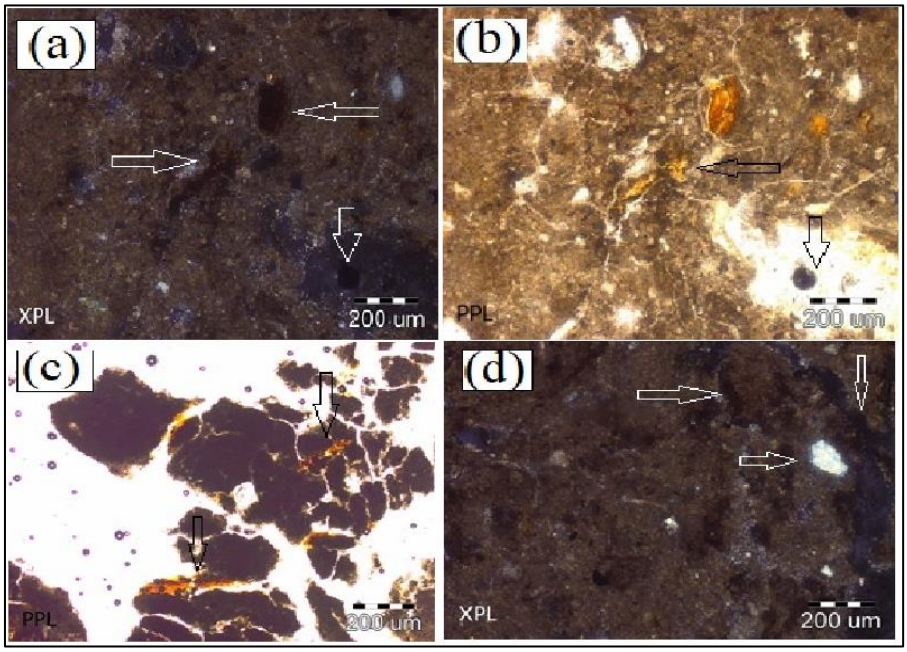

Fig. 10. (a, b) Infilling of voids with rotting root, impregnated feature, and Fe-clay coating in voids (Apg, Pedon 7). (c) Moderately accommodated aggregate with sub angular blocky ped and Fe impregnated with clay coating on ped (Bg, Pedon 7). (d) Infilling of Fe oxides, Fe coating on peds, and quartz minerals in the void (Bg, Pedon 7).

The distribution pattern is predominantly porphyric, although some areas exhibit monic and porphyric characteristics. The coarse materials primarily consist of limestone fragments, whereas the fine fraction comprises thin crystals of iron, manganese, and quartz, along with minor amounts of calcite. The most common b-fabric observed in all thin sections is the crystallitic type (Kemp et al., 2004). Mn and Fe oxides throughout the samples occur as coatings, hypocoatings, quasicoatings, and nodules. The nodules are present in typical and aggregate forms, and only rarely in digitate forms. Impregnated redox pedofeatures represent zones where oxidized Fe and/or Mn have accumulated within the matrix as nodules or as Fe/Mn oxide hypocoatings or quasicoatings along voids or coarse mineral grains, resulting from fluctuations in the oxidation state of these elements. Across all thin sections, the most common pedogenic features are coatings and hypocoatings of iron and manganese oxides.

Nodules and infillings of Fe and Mn oxides are also observed. The abundance of these pedofeatures increases with depth. In some cases, calcite nodules impregnated with iron and manganese are present, consistent with findings reported by Huang et al. (2018), Gasparatos et al. (2019), Raheb and Hydari (2023), and Zhuang et al. (2025). The enhancement of these soil-forming features under flooding conditions can influence the movement and retention of certain elements, such as phosphorus, thereby affecting their availability to plants (Gasparatos et al., 2019). Gray zones resulting from iron depletion, together with various accumulations of iron compounds, are prominent characteristics of paddy soils. These features indicate inadequate drainage associated with mudslides, prolonged surface saturation, and elevated groundwater levels.

CONCLUSION

Changes in macromorphological and micromorphological properties of soils can significantly influence nutrient availability. The studied soils were calcareous and, after approximately 50 years of flooded cultivation, tend to approach neutral pH conditions. This shift may also affect the availability of both micro- and macronutrients. Micromorphological and physicochemical analyses indicated that continuous rice cropping systems over a 50-year period have influenced soil structure and porosity patterns. The presence of weak-to-moderately developed structural units in the surface horizons and massive structures at greater depths suggests soil degradation and compaction resulting from the destruction of rice paddies, which negatively affects plant growth. Furthermore, prolonged cultivation and tillage increase the accumulation of iron and manganese oxides, which can influence the availability of certain elements, such as phosphorus. However, the results also indicate that rice cropping systems combined with upland crops improve soil quality and straw yield in the subsequent season, compared to rice monoculture. Therefore, it is recommended that the concentrations of both low-demand and high-demand nutrient elements be measured before and after flooding, as well as in adjacent intact soils, in order to better evaluate the effect of flooding on the nutrient availability.

FUNDING

This research did not receive any funding.

CRediT AUTHORSHIP CONTRIBUTION STATEMENT

Conceptualization: Soheila Sadat Hashemi, Zahra Pourakbari, and Saeid Hojati; Methodology: Soheila Sadat Hashemi and Zahra Pourakbari; Validation: Soheila Sadat Hashemi and Zahra Pourakbari; Investigation: Soheila Sadat Hashemi, Zahra Pourakbari, and Saeid Hojati; Resources: Soheila Sadat Hashemi and Zahra Pourakbari; Data curation: Soheila Sadat Hashemi and Zahra Pourakbari; Writing—original draft preparation: Soheila Sadat Hashemi; Writing— review and editing: Soheila Sadat Hashemi; Visualization: Soheila Sadat Hashemi; Supervision: Soheila Sadat Hashemi; Project administration: Soheila Sadat Hashemi; Funding acquisition: Soheila Sadat Hashem, Zahra Pourakbari, and Saeid Hojati.

DECLARATION OF COMPETING INTEREST

The authors declare no conflicts of interest.

ETHICAL STATEMENT

The authors avoided from data fabrication and falsification.

DATA AVAILABILITY

The readers are encouraged to contact the corresponding author via email to gain access to the data used in this study.

REFERENCES

Afzaal, M., Mirza, S. A., Mir, M., Ahmed, S., Rasul, A., Nasir, S., & Waqas, M. Y. (2018). In Paddy Soil. *Environmental Pollution of Paddy Soils*, *53*, 99-112. https://doi.org/10.1007/978-3-319-93671-0_6

Allison, L. E., & Moodi C. D. (1965). Carbonates. In Black, C.A. (ed), *Methods of Soil Analysis. Part 2, Chemical and Microbiological Properties*. (pp. 1379-1396). Madison, WI: American Society of Agronomy.

Ayoubi, S., Mosaddeghi, M. R., Yousefifard, M., Vafaeezadeh, R., Shahpouri, F., & Cerda, A. (2025). Soil pore size distribution and quality indicators affected by land use change and slope position, using micromorphology analysis in Southern-West Iran. *Land Degradation & Development*, *36* (16), 5697–5710. https://doi.org/10.1002/ldr.70031.

Banaei, M. H. (1998). Soil moisture and temperature regimes map of Iran. Soil and water research institute of Iran. (In Persian)

Chapman, H. D. (1965). Cation exchange capacity. In Black C. A. (ed), *Methods of Soil Analysis, Part 2, Chemical and Microbiological Properties* (pp. 891-901). WI: Society of American Agronomy, Madison.

Chen, X., Hu, Y., Xia, Y., Zheng, S., Ma, C., Rui, Y., He, H., Huang, D., Zhang, Z., Ge, T., Wu, J., Guggenberger, G., Kuzyakov, Y., & Su, Y. (2021). Contrasting pathways of carbon sequestration in paddy and upland soils. *Global Change Biology*, *27*(11), 2478–2490. https://doi.org/10.1111/gcb.15595

Cheng, Y. Q., Yang, L. Z., Cao, Z. H., Ci, E., & Yin, Sh. (2009). Chronosequential changes of selected pedogenic properties in paddy soils as compared with non-paddy soils. *Geoderma*, *151*, 31-41. https://doi.org/10.1016/j.geoderma.2009.03.016

Gargiulo, L., Mele, G., & Terribile, F. (2013). Image analysis and soil micromorphology applied to study

physical mechanisms of soil pore development: An experiment using iron oxides and calcium carbonate. *Geoderma*, 197–198, 151–160. https://doi.org/10.1016/j.geoderma.2013.01.008

Gasparatos, D., Massas, I., & Godelitsas, A. (2019). Fe-Mn concretions and nodules formation in redoximorphic soils and their role on soil phosphorus dynamics: Current knowledge and gaps. *Catena*, 182, 1041. https://doi.org/10.1016/j.catena.2019.104106

Gee, G. W., & Bauder J. W. (1986). Particle size analysis. In Klute, A. (eds.), *Method of Soil Analysis, part 1, Physical and Mineralogical* (pp. 383-411). Madison, WI: American Society of Agronomy.

Hashemi, S. S., & Asadi, F. (2018). Effect of waterlogging cultivation on physical, chemical and mineralogical characteristics of paddy soils in Doroud area, Lorestan Province. *Applied Soil Research, 6*(1), 112-123. (In Persian)

Huang, L., Jia, X., Shao, M., Chen, L., Han, G., & Zhang, G. (2018). Phases and rates of iron and magnetism changes during paddy soil development on calcareous marine sediment and acid Quaternary red-clay. *Scientific Reports*, *8*, 444. https://doi.org/10.1038/s41598-017-18963-x

Huang, L., & Wang, Y. (2023). Micromorphology, mineralogy, and geochemistry of ferromanganese nodules in tropical soils and their impacts on heavy metal sequestration. *Journal of Cleaner Production*, *383*, 135498. https://doi.org/10.1016/j.jclepro.2022.135498

Kawaguchi, K., & Kyuma, K. (1974). Paddy soils in tropical Asia. Southeast Asian Studies, Part1, Description of Fertility Characteristics. *Southeast Asian Studie*, 1*2*(1), 3-24.

Kemp, R.A., Toms, P.S., King, M., & Krohling, D. M. (2004). The Pedosedimentary evolution and chronology of Tortugas, a Late Quaternary type-site of northern Pampa, Argentina. *Journal of Quaternary International, 114*, 101-112.

Khedri, Z., Hashemi, S. S., & Abbaslou, H. (2018). Investigation of some microscopic features in Canola and Sugar beet long term cultivations. *Journal of Water and Soil Conservation, 24*(6), 283-290. 10.22069/jwsc.2017.13280.2793.

Khokhlova, O., Myakshina, T., & Kuznetsova, A. (2021). Origins of hard carbonate nodules in arable Chernozems in the Central Russian Upland. *European Journal of Soil Science*, *72*(1), 326-342. https://doi.org/10.1111/ejss.12948

KIlfeather, A. A., & Vandermeer, J. M. (2008). Pore size, shape and connectivity in tills and their relationship to deformation processes. *Quaternary Science Reviews, 27*, 250-266. https://doi.org/10.1016/j.quascirev.2006.12.015

KOwalska, J. B., Zaleski, T., & Mazurek R. (2020). Micromorphological features of soils formed on calcium carbonate–rich slope deposits in the Polish Carpathians. *Journal of Maintain Science*, *17*(6), 1310-1332.https://doi.org/10.1007/s11629-019-5829-5

Kyuma, K. (1985). Fundamental characteristics of wetland soils. In: Greenland, D. J., Alcasid, G. N., & Eswaran, H. (Eds.), *Wetland soils: Characterization, classification and utilization*. Los Banos, Philippines: International Rice Research Institute.

Lee, H., French, C., and Macphail, R. I. (2014). Microscopic examination of ancient and modern irrigated paddy soils in South Korea, with special reference to the formation of silty clay concentration features. *Geoarchaeology, 29*, 326–348. https://doi.org/10.1002/gea.21478

Linh, T. B., Sleutel, S., Elsacker, S. V., Goung, V. T., Khoa, L.V., & Cornelis, W. M. (2015). Inclusion of upland crops in rice-based rotations affects chemical properties of clay soil. *Soil Use and Management, 31*, 313-320. https://doi.org/10.1111/sum.12174

Loppert, R. H., & Suarez, D. L. (1996). Carbonate and gypsum. In Sparks, D. L. (Eds.), *Methods of soil analysis, Part III*, (pp. 437- 474). Madison, WI. USA: American Society of Agronomy.

Murphy, C. P. (1986). *Thin section preparation of soils and sediments*. Berkhamsted: Academic Publication.

Nakatsuka, H., & Tamura, K. (2016). Characterization of soils under long-term crop cultivation without fertilizers: A case study in Japan. *Springer Plus 5*(283), 2-22. https://doi.org/10.1186/s40064-016-1917-y

Nakao, A., Takeda, A., Ogasawara, S., Yanai, J., Sano, O., & Ito, T. (2015). Relationships between paddy soil radiocesium interception potentials and physicochemical properties in Fukushima, Japan. *Journal of Environmental Quality*, *44*(3), 780-788. https://doi.org/10.2134/jeq2014.10.0423

Nelson, D. W., & Sommers, L. E. (1996). Total carbon, organic carbon and organic matter. In Sparks, D. L. (Eds.), *Methods of soil analysis, Part III*, (pp. 961-1010). Madison, WI. USA: American Society of Agronomy.

Ponnamperuma, F. N. (1978). *Electrochemical change in submerged soil and the growth of rice*. Los Banos, Philippines: International Rice Research Institute.

Prakongkep, N., Suddhiprakarn Kheoruenromne, I., & Gilkes, R. J. (2007). Micromorphological properties of Thai paddy soils. *Kasetsart Journal (Nat. Sci.)*, 41, 42-48.

Raheb, A. R. & Heidari, A. (2023). Comparison of clay mineralogy and micromorphological image analysis of anaerobic and aerobic soils in the north of Iran. *Eurasian Soil Science*, *56*, 1463–1478. https://doi.org/10.1134/s1064229323600355Rhoades, J. D. (1996). Salinity: Electrical conductivity and total dissolved solids. In Sparks, D. L. (Eds.), *Methods of soil analysis, Part 3, 3rd Ed.*, (pp. 417-436). Madison, WI: American Society of Agronomy.

Roquero, E., Silva, P. G., Zazo, C., Goy, J. L., Dabrio, C. J., & Borja, F. (2013). Micromorphology of hydromorphic soils developed in fluvio-marine sediments during the Middle-Late Pleistocene transit in the Gulf of Cadiz (Atlantic South Spain). *Spanish*

Journal of Soil Science, 3(3),184-200. https://doi.org/10.3232/sjss.2013.v3.n3.04

Soil Survey Staff. (2022). *Keys to soil taxonomy* (No. Ed. 12). Washington DC: United States Department of Agriculture, Natural Resources Conservation Service.

Stoops, G. (2003). *Guidelines for analysis and description of soil and regolith thin section*. Madison: Soil Science Society of America.

Thomas, G. W. (1996). Soil pH and soil acidity. In Sparks, D. L. (ed.), *Methods of Soil Analysis, Part 3, 3rd Ed.*, (pp. 475-490). Madison, WI: American Society of Agronomy.

Vera, M., Sierra, M., Diez, M., Sierra, C., Martinez, A., Martinez, F. J., & Aguilar, J. (2007). Deforestation and land use effects on micromorphological and fertility change in acidic rainforest soils in Venezuelan Andes. *Soil and Tillage Research, 97*, 184-194. https://doi.org/10.1016/j.still.2007.09.015

Witt, C., & Haefele, S. M. (2005). Paddy soil. In Hillel, D., Rosensweig, C., Powlson, D., Scow, K., Singer, M., & Sparks, D. (Eds.), *Encyclopedia of Soils in the Environment*. New York: Academic Press.

Wu, B., Meng, X., Yao, H., & Amelung, W. (2024). Iron dynamics and isotope fractionation in soil and rice during 2000 years of rice cultivation. *Plant Soil, 495*, 615–629. https://doi.org/10.1007/s11104-023-06352-5

Xia, X., Yang, Z., Xue, Y., Shao, X., Yu, T., Hou, Q. (2017). Spatial analysis of land use change effect on soil organic carbon stocks in the eastern regions of China between 1980 and 2000. *Geoscience Frontiers, 8(3), 597–603.* https://doi.org/10.1016/j.gsf.2016.06.003

Yurong, H. E., Chengmin, H. U., Xiangming, X. U., Yanqiang, W. A., & Xiubin, H. E. (2008). Micromorphological features of Paleo-Stagnic-Anthrosols at archaeological site of Sanxingdui. *China Journal of Mountain Science, 5*, 358-366. https://doi.org/10.1007/s11629-008-0220-y

Zhuang, Y., Ding, P., Zhuang, L., Wang, Y., Wu, W., Wang, X., Niu, Y., Sun, G., Wei, X., & Qin, L. (2025). Geoarchaeological study of the evolution of rice farming fields in prehistoric Yangtze delta and Huai River region of China. *Quaternary Science Reviews, 356*, 109293. https://doi.org/10.1016/j.quascirev.2025.10929